OUT-OF-PLANE SHEAR BEHAVIOR OF SC COMPOSITE STRUCTURES

Amit H. Varma[1], Kadir C. Sener[2], Kai Zhang[3], Keith Coogler[4], Sanjeev R. Malushte[5]
[1]Assoc. Pro., Bowen Lab., School of Civil Eng., Purdue Univ., W. Lafayette, IN. ahvarma@purdue.edu
[2]Ph.D. Candidate, Bowen Lab., School of Civil Eng., Purdue Univ., W. Lafayette, IN. ksener@purdue.edu
[3]Ph.D. Candidate, Bowen Lab., School of Civil Eng., Purdue Univ., W. Lafayette, IN. kai-z@purdue.edu
[4]Sr. Engineer, Westinghouse Elec. Corp., Cranberry Township, PA. cooglekl@westinghouse.com
[5]Bechtel Fellow and Sr. Principal. Engineer, Bechtel Power Corp., Frederick, MD, USA, smalusht@bechtel.com
E-mail of corresponding author: ahvarma@purdue.edu

ABSTRACT

Steel-plate composite (SC) walls of safety-related nuclear facilities are subjected primarily to in-plane shear forces and gravity loads. They are also subjected to out-of plane shear and bending demands closer to the foundation regions and at connections or interfaces with other structures. The out-of-plane behavior of SC walls is not well understood, but it is expected to be similar to the behavior of RC walls.

The out-of-plane behavior of RC walls is influenced by several parameters including the section depth, rebar ratio, spacing, and size of out-of-plane shear reinforcement. These parameters are expected to have a similar influence on the out-of-plane behavior of SC walls. The out-of-plane behavior of steel-concrete composite walls was evaluated by conducting one-way bending tests on beams that were representative of a large scale wall design in the longitudinal and transverse directions. The SC beam specimens were tested in both three and four-point bending tests with concentrated forces applied at distance (a) from the simple supports.

Several SC beam specimens were tested with different shear span-to-depth (a/d) ratios, steel plate thickness (reinforcement ratio), shear stud spacing, and in the presence or absence of shear reinforcement. This paper summarizes the results of the experimental investigations including the load displacement responses and comparisons with equations that are in the current design codes. The paper also includes the results of detailed 3D finite element analyses of the specimens, and observations of behavior based on experimental and analytical results.

INTRODUCTION

SC walls are being considered for use in nuclear power plant construction due to their economic advantages over conventional reinforced concrete construction. These economic benefits of SC construction are due to their potential short construction duration and added efficiency of having steel plates surrounding the concrete portion. So far, this added efficiency has been demonstrated for blast and missile resistance, and in-plane shear strength with the recent SC wall related research [4, 5].

Out-of-plane shear strength of SC designs have been addressed in JEAG 4618 [3] technical guidelines based on some previous research that involved testing of beams having a/d ratios as large as 2.6 and depths less than 26 in. [6]. At these smaller a/d ratios, D region effects [8] are seen in the load carrying mechanism such as compression struts or arching action which tend to overestimate the lower bound shear strength of the SC design. Therefore in this study the shear span-depth ratio has been mostly kept above 3 to capture the lower bound strength values.

Another objective of this paper is to evaluate whether the out-of-plane shear strength of SC design that is only subjected to shear and flexure can be conservatively estimated using ACI code provisions for shear strength of reinforced concrete beams. ACI 349 [1] references the ACI 318 [2] code provisions for shear strength, which are summarized using Equations 1 through 3. In these equations the total shear strength (V_n) is given as summation of two parts where V_c is the shear strength contribution of the concrete and V_s is the shear strength contribution from the shear reinforcement that is used such as using deformed bar or wire reinforcement.

$$V_n = V_c + V_s \quad (1)$$

$$V_c = 2\sqrt{f'_c}\, A_c \quad (2)$$

$$V_s = A_v f_{vt} \frac{d}{s} \quad (3)$$

In these equations; f'_c is the compressive strength of concrete, A_c is the cross-sectional area of concrete, F_{vt} is the yield strength of vertical shear reinforcement, A_v is the cross-sectional area of shear reinforcement, d is the section depth, and s is the shear reinforcement spacing.

An experimental test program has been carried out to determine the out of plane shear behavior and also to evaluate the conservatism of above equations to SC out-of-plane shear design. A total of eight adequately instrumented SC design simply supported beams have been tested. The depth-to-shear span ratios for tested specimens ranged from 2.5 to 5.5. Shear studs welded to the steel plates transferred the interfacial (horizontal) shear force that occurs between the concrete and steel portions due to bending. The vertical shear force, which is independent from the horizontal shear strength, is transferred by concrete and steel shear reinforcement (if provided).

The vertical shear force transfer in concrete occurs due to combination of different load carrying mechanisms such as; shear resistance in the uncracked compression zone, aggregate interlock on the crack interface and dowel action of longitudinal reinforcement. Adding transverse shear reinforcement also has an influence on each of these load carrying mechanisms in concrete. In order to investigate these phenomenon and the effects of shear reinforcement, the test specimens were categorized into two major sets. The first set of specimens did not have any transverse tie-bars or shear stirrups. The second set had shear reinforcement in the form of transverse tie bars included. Parameters that were varied in both set of tests were similar; for example; a/d ratios, steel plate thickness, shear stud spacing and specimen size. Additionally, the test results were supported by computational results obtained from 3D nonlinear inelastic finite element (NIFE) analyses of the specimens.

EXPERIMENTAL AND ANALYTICAL INVESTIGATION OF BEAMS WITHOUT SHEAR REINFORCEMENTS (V_C)

Five simply supported SC beam specimens without any out-of-plane shear reinforcement were tested to experimentally determine their out-of-plane shear strength. These specimens SP1-1 to SP1-5 are summarized in Table 1.

- The first four specimens (SP1-1 to SP1-4) had similar overall geometric dimensions. These specimens had 18 in. depth and 12 in. width and 8 or 10 ft. length. They were subjected to three-point bending loading as illustrated in Figure 1 for Specimen SP1-1. The variables among these four tests were shear stud spacing, steel plate thickness and the shear span ratio.
- The fifth specimen (SP1-5) in this set was subjected to four-point bending. Specimen SP1-5 had 36 in. depth, 34¼ in. width and 33 ft. length. This specimen represented full scale geometric dimensions in terms of what is used in the current SC construction for nuclear applications.

Concrete infill used for all five specimens were 6 ksi self-consolidating concrete with maximum aggregate size being ¾ inches. Due to the size difference of the last specimen the shear stud size and length was scaled up for that specimen. The shear studs that were used in the first four specimens were 0.5 in. dia x 2.5in. long studs (Stud1). For specimen SP1-5 the shear studs were 0.75in. dia x 6in. long studs (Stud2). The geometric details of the specimens are given in Table 1. The concrete strengths for specimens were measured on the day of test.

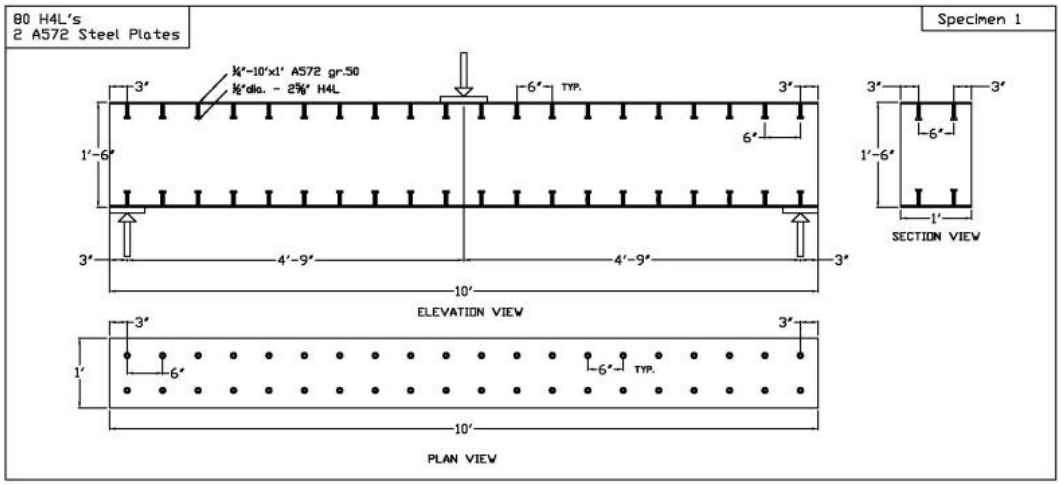

Figure 1 – Specimen Drawing for SP1-1

Table 1 – Details of Test Specimens without Shear Reinforcement

Specimen	L, (in)	b_w, (in)	t_s, (in)	d_c, (in)	a_v/d	s, (in)	*Shear stud type*	ρ, (%)	f'_c (ksi)	F_{y_plate} (ksi)	F_{y_stud} (ksi)	Loading Method
SP1-1	120	12	0.25	17½	3.20	6	Stud1	1.43	6.1	65	70.9	3-point
SP1-2	120	12	0.25	17½	3.25	12	Stud1	1.43	6.1	65	70.9	3-point
SP1-3	120	12	0.375	17¼	3.20	6	Stud1	2.08	6.1	65	70.9	3-point
SP1-4	96	12	0.25	17½	2.50	6	Stud1	1.43	6.1	65	70.9	3-point
SP1-5	396	34¼	0. 5	35	3.50	10	Stud2	1.43	6.2	71	71	4-point

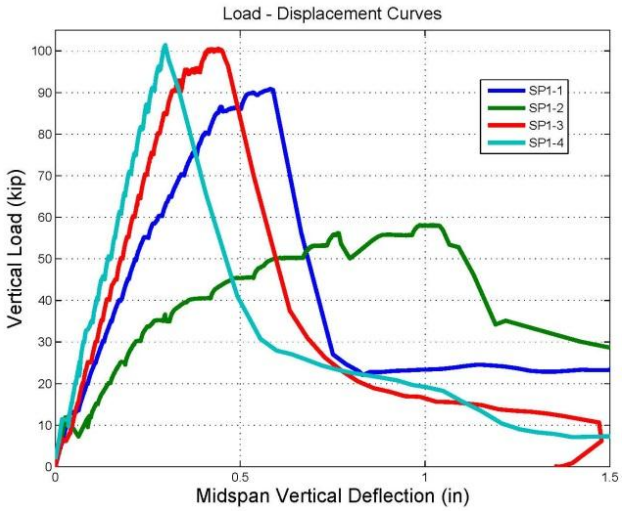

Figure 2 – Load vs. Mid-span Deflection Curves for SP1-1, SP1-2, SP1-3 and SP1-4

Figure 2 shows the load displacement curve for the first four specimens (SP1-1 to SP1-4) that did not have any shear reinforcement. The corresponding experimental results are shown in Table 2. Table 2 includes the force levels corresponding to the appearance of visible flexural cracking, diagonal shear cracking, and shear failure. It also includes the section plastic moment capacity (M_p) for the specimens, where M_p has been calculated according to JEAG 4618 [3] using Equation 4.

$$M_p = A_s \times F_y \times \frac{7}{8}(d - t_s) \quad (4)$$

In Equation 4, A_s is the area of a steel faceplate, F_y is the measured yield stress of the faceplates, d is the section depth and t_s is the faceplate thickness.

Table 2 –Summary of Experimental Results for SP1 Specimen Series without Shear Reinforcement

Specimen	Failure Mode	Flexural Cracking (kips)	Diagonal Shear Cracking (kips)	Maximum Load P_{test} (kips)	Maximum mid-span displacement Δ_{test}, (in)	V_c (eq.2) (kip)	M_p (eq.4) (kip-in)	V_{test}, (kip)	M_{test} (kip-in)	$\frac{V_{test}}{(b_w d\sqrt{f'_c})}$,	$\frac{V_{test}}{V_c}$
SP1-1	Mode1	14	80	91	0.58	32.8	3119	45.4	2600	2.77	1.38
SP1-2	Mode2	12	--	58	1.00	32.8	3119	29	1697	1.77	0.88
SP1-3	Mode1	5	95	100	0.35	32.3	4678	50	2875	3.09	1.55
SP1-4	Mode1	12	80	102	0.30	32.8	3119	51	2321	3.11	1.56
SP1-5	Mode1	25†	131†	177†	1.00	186	53404	177	22302	1.90	0.95

† Values are calculated as the average of the force applied by two load rams

As shown in Table 2 and Figure 2, all the specimens SP1-1 through SP1-5 failed in a sudden and brittle manner due to shear failure. None of these specimens developed flexural failure, which is evident from the fact that the applied moment at failure (M_{test} in Table 2) is significantly lower than the plastic moment capacity (M_p) of the specimen. As shown in Table 2, flexural cracks appeared in all the specimens as soon as the hydraulic ram got in contact with the specimens, which takes place at about 5-10% of the maximum load. This indicates how quickly the transition to cracked section occurs.

All the specimens (except SP1-2) failed in vertical shear due to the formation of diagonal shear cracks (Mode1). Specimen SP1-2 failed in interfacial (horizontal) shear (Mode 2) at the steel plate / concrete interface, because it was designed with insufficient number of studs in the shear span. This Specimen SP1-2 also had lower stiffness due to the significantly reduced composite action between the steel plates and the concrete, and failed by excessive end slip and fracture of all the studs in the shear span.

The vertical shear failure modes for Specimens SP1-1, SP1-3, and SP1-4 were similar to the failure mode presented in JEAG 4168 for beams having a/d=2.6. The concrete crack maps for SP1-1 and SP1-3 are shown in Figure 3. The crack map for SP1-4 is shown in Figure 4. Additionally, Figure 5 shows an example crack map of the failure mode reported in JEAG 4618 for beams with a/d = 2.6. As shown, the concrete crack maps in Figures 3 and 4 agree with that shown in Figure 5.

Using the thicker steel plate for SP1-3 resulted in a slight increase (10%) in the peak load, but it still had the same failure mode as SP1-1 (see Figure 3). Similarly the smaller shear span ratio for SP1-4 resulted in slightly higher load capacity. As seen in Table 2, the diagonal shear cracks formed around the same load levels for both SP-1 and SP1-4, but SP1-4 had slightly higher shear failure strength due to influence of D-region effects. This indicates that the lower bound out-of-plane shear strength for SC design should be obtained by testing beams with a/d ratios greater than 3, as opposed to 2.5, which is more applicable for reinforced concrete design.

Figure 6 shows the crack distribution map for the large-scale Specimen SP1-5 (depth = 36 in.). As mentioned earlier, this specimen was subjected to four-point loading. The crack pattern shown in Figure 6 corresponds to flexural shear cracking that is slightly different from those shown in Figures 3-5 (diagonal shear cracking). Additionally, the crack pattern in Figure 6 does not extend to the supports. There is clear difference in the behavior, cracking, and failure of SP1-5 (large depth and four point loading) as compared to Specimens SP1-1 to SP1-4 (smaller depth and three point loading).

Table 2 includes comparisons of the experimental shear strength (V_{test} in Table 2) with the values calculated using ACI code (Equation 2). As shown, SP1-1, SP1-3, and SP-4 had out-of-plane shear strength (V_{test}) greater than the value (V_c) calculated using the ACI code. Specimen SP1-2 failed in interfacial shear, and the ACI code equation for vertical shear failure does not apply for it. The shear strength (V_{test}) of SP1-5 was slightly lower than the value (V_c) calculated using ACI code (Equation 2) probably due to size or scale effects. In general, the out-of-plane shear strength of the tested specimens was predicted reasonably using ACI code equations.

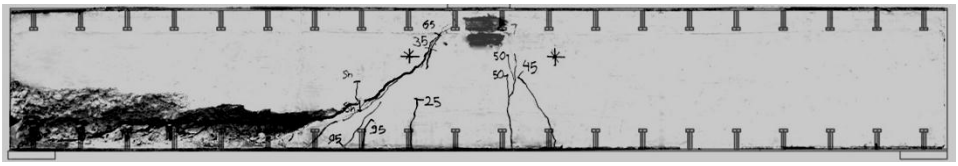

Figure 3 – Concrete crack map and failure mode for SP1-1 & SP1-3

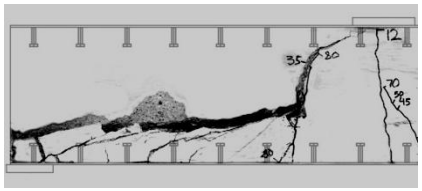

Figure 4. Cracking & failure mode for SP1-4

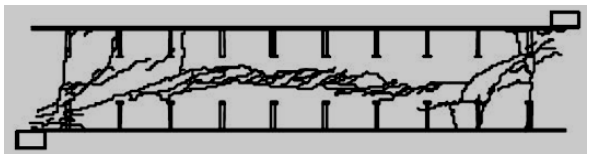

Fig. 5. Failure mode for beam with a/d =2.6 in. JEAG 4618

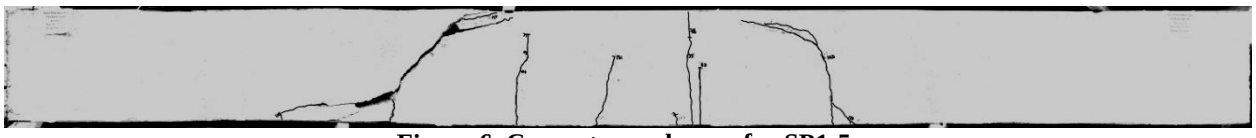

Figure 6. Concrete crack map for SP1-5

Overall Approach for Analytical Investigation

3D nonlinear inelastic finite element (NIFE) models of the tested specimens were developed and analyzed using ABAQUS [7], which is a commercially available finite element analysis program. The brittle behavior of concrete in tension makes it almost impossible to obtain converged results in standard (predictor-corrector) analysis methods like full Newton or modified Newton-Raphson. Therefore the explicit dynamic analysis method was used for all the analyses presented here. The primary advantage and reason for using this method is that it can find results

close or even slightly beyond failure, particularly when brittle materials (like concrete in tension) and failures are involved.

The explicit dynamic analysis method was used to perform quasi-static analyses simulating the experiments. To make sure that the response is quasi-static the system kinetic energy in the model was monitored constantly and kept below 5% of the system internal energy. Also mass scaling was used to increase the analysis time steps and to obtain results in a timely manner. The analyses were performed using ABAQUS and the program built-in material models were used with parameters associated to each material used in specimens.

The concrete material model was chosen to be the brittle cracking model (CEF) mainly due to its more advanced cracking features and also having the element deletion feature once an element completely loses its load carrying capacity. The CEF model assumes linear elastic behavior for the concrete in compression. The tension behavior of the concrete can be specified using either its fracture energy (G_f), or associated tension stress-crack opening displacement curve. Also the shear retention behavior can be specified directly with linear or exponential degradation and a tensile (crack opening) strain (ε).

For simplicity and consistency both the tension stiffening and the shear retention curves are chosen to be linearly degrading to the same crack opening displacement value. Fig. shows the tension stress-crack opening displacement curve that was calibrated for the experiments presented here. Steel behavior is modeled using multiaxial plasticity theory with: (i) Von Mises yield surface, (ii) associated flow rule, and (iii) isotropic hardening. The uniaxial stress-strain curve in tension and the poisson's ratio were the only input data required to completely define the multiaxial plasticity model for the steel portions.

Figure 8 shows a comparison of the experimentally measured and analytically predicted load (shear) – displacement responses for Specimen SP1-5. The analytical predictions were obtained using the 3D NIFE models and analyses described here. As shown in the figure, the NIFE models also predict brittle shear failure at the peak load because of the cracked concrete losing its shear carrying ability. The horizontal line in the figure corresponds to V_c calculated using ACI code equations [Equation (2)]. As shown, the specimen failed just before reaching V_c.

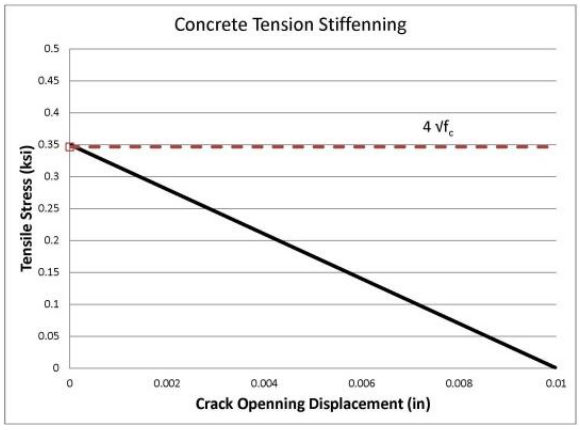

Fig. 7. Tension Stiffening Curve used for the Analysis

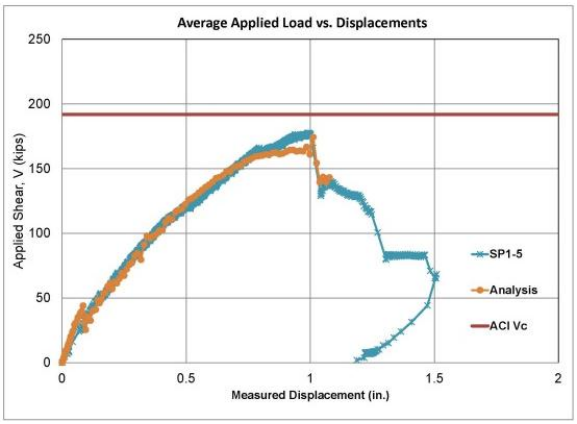

Fig. 3 - Load vs. displacement curves for SP1-5

EXPERIMENTAL AND ANALYTICAL INVESTIGATION OF BEAMS WITH SHEAR REINFORCEMENTS (V_C+V_S)

Three large-scale out-of-plane shear tests were conducted to evaluate the effects of including shear reinforcement and the conservatism of the ACI code equations [Equations 1-3] for SC design. The tests were conducted by subjecting full-scale SC beam specimens to four-point bending as shown in Figure 4. The specimens had roller supports and were subjected to concentrated forces at two load points. The mid-span regions of the specimens were subjected to uniform moment, while the spans closer to the supports were subjected to uniform shear. The distance between the supports and the load points is designated as the shear span (a). Each specimen had same specimen cross-section, tie bar diameter and spacing, and shear stud diameter and spacing but had different shear span-to-depth (a/d) ratios of 2.5, 3.5, and 5.5, respectively. The concrete infill used for specimens was 7 ksi regular concrete with maximum aggregate size being 1.5 inches. Geometric and material properties of the specimens are summarized in **Analytical Investigations**

.

The load-displacement responses for specimens SP2-1 and SP2-2 are shown in Figures 10 and 11. These figures include horizontal lines indicating the shear strengths (V_c; and V_s+V_c) calculated using measured concrete

and measured steel material properties for the tie bars. As shown, the shear strength of the specimens SP2-1 and SP2-2 is greater than that estimated using ACI code equations [Equations 1-3]. There is some nonlinearity in the force-deflection responses due to concrete cracking and steel tie bar yielding close to the peak load. As expected, the maximum load capacity (430 kips) of the Specimen SP2-2 with a/d =2.5 is slightly (13%) greater than that for Specimen SP2-1 with a/d = 3.5 (380 kips). Specimen SP2-2 with a/d=2.5 has smaller bending moments and perhaps some arch action effects that are relatively absent in Specimen SP2-1 with a/d=3.5.

Table 3 - Details of test specimens with shear reinforcement

Specimen	Depth	Length	Width	Steel Plate Thick	Shear Span a/d	Stud spacing	Tie Bar spacing	Stud	Tie Bar	$\rho = 2t_s/T$ %	f'_c (ksi)	F_{y_plate} (ksi)	F_{y_stud} (ksi)	$F_{y\_tie\_bar}$ (ksi)
SP2-1	T	11 T	0.96 T	t_s	3.5	¼ T	½ T	dia = t_s length = T/6	dia = t_s length = T	4.2	7	58	61.5	83.5
SP2-2	T	7 T	0.96 T	t_s	2.5	¼ T	½ T	dia = t_s length = T/6	dia = t_s length = T	4.2	7.6	62	61.5	83.5
SP2-3	T	13.3 T	0.96 T	t_s	5.5	¼ T	½ T	dia = t_s length = T/6	dia = t_s length = T	4.2	7.5	56	61.5	83.5

Figure 12 shows the load – displacement response for Specimen SP2-3 with a/d=5.5. The figure includes horizontal lines corresponding to the shear strength and moment capacity (Mp) calculated using measured material properties. As expected, this specimen developed its flexural capacity with extensive yielding of the bottom steel plate. Shear failure did not occur for this specimen.

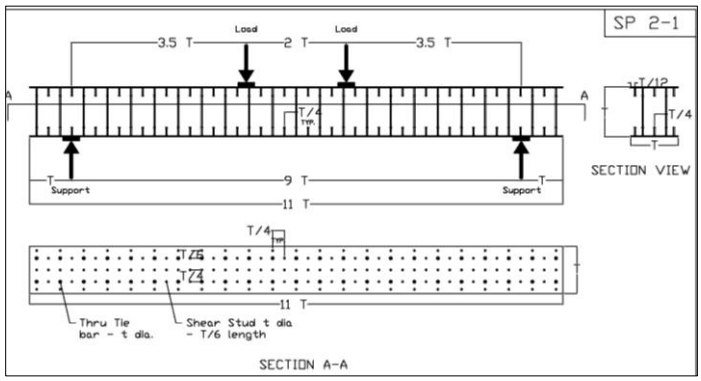

Figure 4 –Specimen Drawing for SP2-1

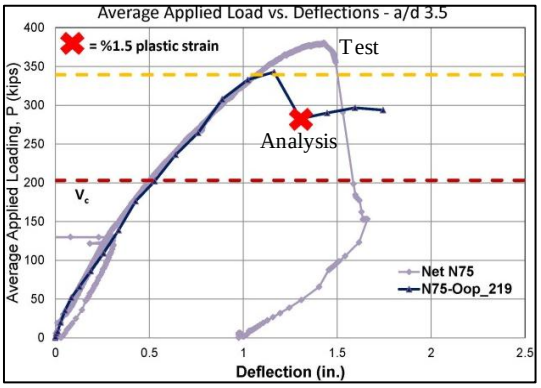

Figure 10 Load – displacement response of SP2-1

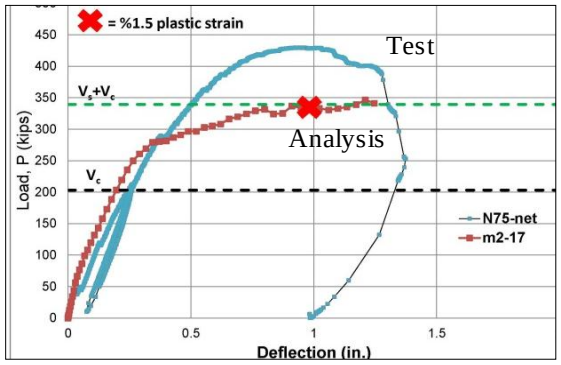

Figure 11 Load – displacement response of SP2-2

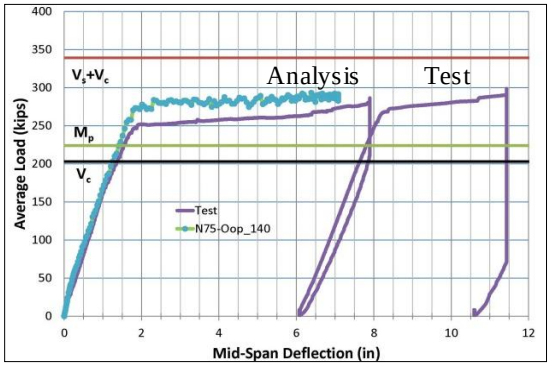

Figure 12 Load – displacement response of SP2-3

Figure 13 shows the concrete cracking map for Specimen SP2-1 with a/d=3.5. The cracking pattern reflects the occurrence of flexural cracking in the midspan (uniform moment region), and flexural shear cracking leading to eventual shear failure of the specimen in the shear spans. As expected, the concrete cracking map in Figure 13 is similar to that shown in Figure 6 for the similar Specimen SP1-5 without any shear reinforcement.

Figure 14 shows the concrete cracking map for Specimen SP2-2 with a/d=2.5. This cracking pattern also reflects the occurrence of flexural cracking in the midspan (uniform moment region), and diagonal shear cracking leading to eventual shear failure of the specimen in the shear spans. Figure 15 shows the concrete cracking map for Specimen Sp2-3 with a/d=5.5. The cracking pattern reflects flexural cracking in the midspan and some flexural shear cracking in the shear spans. This specimen developed flexural yielding failure.

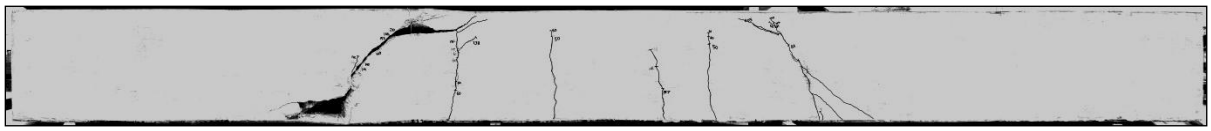

Figure 13 – Concrete crack map for SP2-1

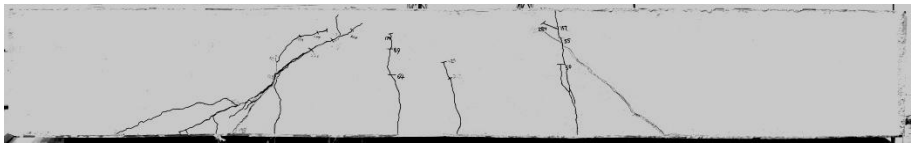

Figure 14 – Concrete Crack Map for SP2-2

Figure 15 – Concrete Crack Map for SP2-3

Analytical Investigations

3D NIFE models of the tested specimens SP2-1 to SP2-3 were developed and analyzed using ABAQUS for the same loading and boundary conditions as the experiments. The models were identical to those described earlier, with the addition that the steel shear reinforcement was also modeled explicitly. The steel material model for the shear reinforcement was the same as that for the steel plates and studs, but it utilized the measured material properties (stress-strain curve) for the tie bars. Additionally, the plastic strain value corresponding to the fracture failure of tie bars was calibrated using experimental measurements and results.

The load – displacement responses predicted by the 3D NIFE models are included in Figures 10, 11, 12 for Specimens SP2-1, SP2-2, and SP3-3. As shown, the predicted responses compare reasonably with the experimental load-displacement responses. The occurrence of tie bar fracture failure is indicated on the load displacement responses.

The experimental and analytical results show that the concrete cracks cross the steel tie bars and the out-of-plane shear forces are resisted by the tie bars in tension and the cracked concrete in compression. The maximum shear strength of the specimen is reached because the tie bars yield and achieve their stress capacity in tension. As seen in Figure 14, specimen SP2-2 had almost 45 degree diagonal tension cracking in the concrete primarily due to shear force effects. Figure 16 shows the localized tension fracture failure of the Specimen SP2-1 (a/d=3.5) tie bars. Figure 17 shows the diagonal crack pattern in the concrete from the finite element analysis of Specimen SP2-2 (a/d=2.5). It also shows the fracture failure of the tie bars that the diagonal cracks pass through.

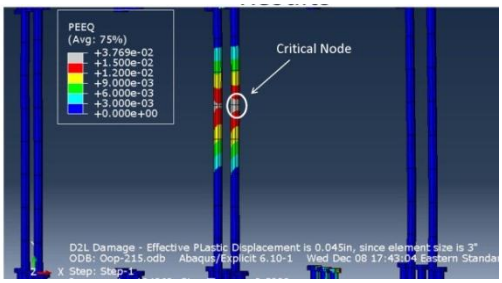

Fig. 16. Facture failure of tie bars in SP2-1 NIFE model.

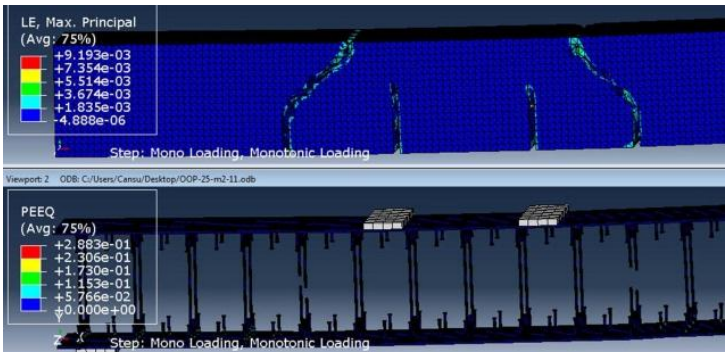

Fig. 17. Concrete cracking and tie bar fracture in NIFE model of SP2-2

SUMMARY AND CONCLUSIONS

A total of eight large-scale SC beam specimens were tested to determine their out-of-plane shear strength. Five specimens were tested without any shear reinforcement, and three with shear reinforcement in the form of tie bars. The parameters included in the experimental investigations were the section depth (T), steel plate thickness (t_s), reinforcement ratio ($2t_s/T$), and shear span ratio (a/d = 2.5 – 5.5).

3D NIFE models were developed and calibrated using experimental results to gain additional insight into the behavior and failure of the tested specimens. The analytical and experimental results were compared with the ACI code [1, 2] out-of-plane shear strength equations for equivalent reinforced concrete beams. The ACI code includes equations for calculating the contributions of both the concrete and the steel tie bars to the shear strength.

The experimental and analytical results indicate that for the specimens tested as part of this research program, the out-of-plane shear strength of SC beams with or without shear reinforcement can be estimated using ACI code equations for RC beams. Additional research is needed to further evaluate and confirm this finding for a wide range of parameters, and including cyclic loading effects and concurrent axial tension effects.

In order to determine the lower bound shear strength for SC beams, it is recommended that the out-of-plane shear tests be conducted for shear span ratios greater than 3. It is evident that include shear reinforcement significantly alters the shear strength and failure mode of the SC beams as expected. The calibrated 3D NIFE models compare reasonably with the experimental results, and provided additional insight into behavior, force transfer, and failure mechanisms. They are recommended for further research.

ACKNOWLEDGMENTS

Testing at Purdue University was partially funded by Westinghouse Electric Company LLC and also partially funded by Bechtel Corporation. All opinions expressed in this paper are strictly those of the authors.

REFERENCES

[1] ACI 349 (2006), "Code Requirements for Nuclear Safety-Related Concrete Structures and Commentary," American Concrete Institute, Farmington Hills, MI.

[2] ACI 318 (2005), "Building Code Requirements for Structural Concrete and Commentary," American Concrete Institute, Farmington Hills, MI..

[3] JEAG 4618 (2005). "Technical Guidelines for Seismic Design of Steel Plate Reinforced Concrete Structures: Buildings and Structures," *Japanese Electric Association Nuclear Standards Committee*, Tokyo, Japan

[4] Mizuno, J., Koshika, N., Sawamoto, Y., Niwa, N., Yamashita, T., Suzuki, A., (2005). "Investigations on Impact Resistance of Steel Plate Reinforced Concrete Barriers against Aircraft Impact Part 1: Test Program and Results", *Transactions of the 18th International Conference on Structural Mechanics in Reactor Technology (SMiRT-18)*, Vol. J J05/1.

[5] Ozaki, M., Akita, S., Niwa, N., Matsuo, I., Usami, S., (2001), Study on Steel Plate Reinforced Concrete Bearing Wall for Nuclear Power Plants Part 1; Shear and Bending Loading Tests of SC Walls, *16th International Conference on Structural Mechanics in Reactor Technology (SMiRT-16).*

[6] Takeuchi, M, Fujita, F., Funakoshi, A., Shohara, R., Akira, S., and Matsumoto, R., (1999). "Experimental Study on Steel Plate Reinforced Concrete Structure, Part 28 Response of SC Members Subjected to Out-of-Plane Load (Outline of the Experimental Program and the Results)." *Proceedings of the Annual Conference of Architectural Institute of Japan*, (in Japanese), pp 1037- 1038, 1999

[6] Abaqus (2010). Analysis Theory Manual - version 6.10. Dassault Systèmes.

[8] Wight J.K., MacGregor, J.G. (2008). *Reinforced concrete: Mechanics and Design*. 5th Edition. Prentice-Hall, NJ.